

Mechanistic Approach for Relating Test Roller Penetration to Strength Properties of Bases and Subgrades

James P. Hambleton
(Corresponding Author)
Graduate Research Assistant
Department of Civil Engineering
University of Minnesota
500 Pillsbury Drive S.E.
Minneapolis, MN, USA 55455
Tel: (612) 626-1538
Fax: (612) 626-7750
Email: hamb0025@umn.edu

Andrew Drescher
Professor
Department of Civil Engineering
University of Minnesota
500 Pillsbury Drive S.E.
Minneapolis, MN, USA 55455
Tel: (612) 625-2374
Fax: (612) 626-7750
Email: dresc001@umn.edu

Submission date: July 27, 2007

Total paper length:
(words in text) + 250(number of figures) = 3724 + (250)(10) = 6224

Submitted to the Transportation Research Board
for presentation and publication

Mechanistic Approach for Relating Test Roller Penetration to Strength Properties of Bases and Subgrades

ABSTRACT

Theoretical formulas that relate penetration depth of a test roller to strength properties of bases and subgrades are presented. The algebraic expressions, derived using the generalized bearing capacity formula employed regularly in geotechnical practice, specifically relate angle of internal friction and soil cohesion to the penetration depth of a towed, rigid wheel with a known force (weight) applied. The existence of such a relationship has the potential to reinvent test rolling as a quality assurance tool capable of providing a continuous record of in situ soil strength measurements along a roadway. Besides supplying a means for interpretation of test roller measurements, the proposed formulas provide a method for practitioners to investigate the influence of modifying test roller characteristics (such as reducing weight or changing wheel size) and to calibrate a test roller to be particularly sensitive to certain soils. The predictions show promising agreement with results from three-dimensional numerical simulation and experimental data.

INTRODUCTION

Test rolling is a technique used for quality assurance testing in road construction practice. In this test, a heavy vehicle is operated on a newly constructed roadway embankment, and the penetration depth of the wheels is subsequently used as a measure of soil consistency on a pass/fail basis. This test may be performed on the base or subgrade layers of the embankment, possibly with successive tests for various lifts of placed material.

Test rolling specifications vary widely between regions in the U.S., with some localities abstaining from the practice altogether. Some areas have provisions for “proof rolling” in place of those for “test rolling.” Following Croveti [1], test rolling is distinguished from proof rolling primarily by the type of equipment used. A test roller utilizes a vehicle with narrow, widely-spaced wheels such as a standard dump truck. A proof roller is typically a smooth-drum or rubber-tire roller and, in contrast to test rolling, is intended to correct minor compaction inadequacies in addition to identifying weak areas.

A test roller in present practices across the U.S. is typically a loaded dump truck weighing a total of 180 to 360 kN (20 to 40 tons). Specifications are often vague about how and where penetration depth should be recorded, and acceptance criteria are commonly left to the discretion of field engineers. When specified, acceptable penetration depths range from practically zero to around 80 mm (3 in.). The Minnesota Department of Transportation [2] stipulates use of a specialized two-wheeled trailer weighing 267 kN (30 tons) that is towed behind a tractor (Figure 1). Wheel penetration depths less than 50 mm (2 in.) are considered acceptable, except that an additional 25 mm (1 in.) is allowed in the case of granular soils to be stabilized after test rolling. Photographs of ruts left in passing and failing regions of granular material are in Figure 2.

Presently, a quantifiable relationship between test roller penetration depth and soil mechanical properties does not exist. Current test rolling acceptance criteria have been

determined empirically at best. The procedure is often regarded simply as a method for recognizing severely deficient areas, despite the conceptual elegance embedded in the approach. In fact, one easily obtains from test rolling a continuous record of measurement along the length of an embankment. What remains is to interpret such a record in terms of soil mechanical properties, and this missing piece is precisely the motivation of this paper.

The focus of this paper is on establishing a theoretical relationship between wheel penetration depth and soil strength properties using soil mechanics-based models. In present practice, soil strength is indeed what most test rollers are equipped to measure (as opposed to stiffness for example), as vehicle weights are so large as to induce deformation that is predominantly plastic. The results presented here are an extension of previous work by the authors on purely cohesive soils [3,4]. Research on soil-wheel interaction has also been conducted within the broad field of terramechanics (cf. [5-9]). However, accurate prediction of wheel penetration depth has not played a central role in terramechanics, and methods are historically empirical.

The analysis presented in this paper pertains to a towed, rigid wheel operating on cohesive/frictional soil. The assumption of a towed wheel, for which no torque is transmitted at the axle, is not restrictive, since such wheels are readily available for the purpose of test rolling. Examples include trailer wheels and the steorage wheels on dump trucks. The assumption of a rigid wheel is valid for stiff and highly inflated pneumatic tires [5], and rigid wheels may be easily implemented with specialized test rolling devices such as the one used in Minnesota. Regarding test rolling practice, wheel flexibility only obscures field measurements and complicates the analysis. Furthermore, the simplest case of a right-cylindrical wheel geometry is considered, which reasonably approximates the shape of many tires (e.g., the one shown in Figure 1).

Models are presented for both indentation and rolling processes. The indentation process plays a role when a wheel first enters a region of weak soil, and in the proposed models, rolling is treated as an extension of indentation.



FIGURE 1 Example of test rolling device specified by the Minnesota Department of Transportation [2].

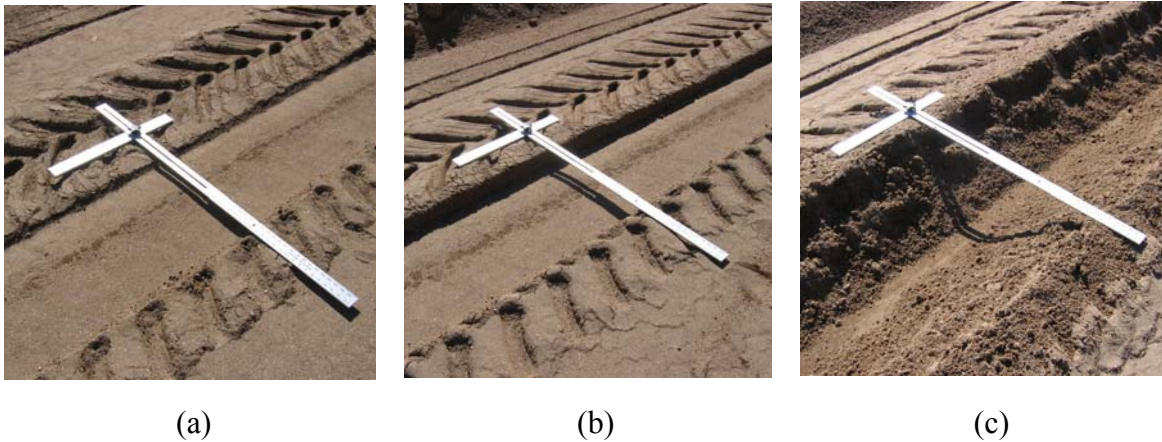


FIGURE 2 Ruts left by test roller in granular soil (square shown in photographs is 1.27 m × 0.56 m): (a) passing soil; (b) soil near failing; (c) drastically failing soil.

THEORETICAL MODELS

In the proposed theoretical models, it is assumed that indentation can be regarded as a sequence of plastic states in the soil and that these plastic states are analogous to those beneath shallow footings at ultimate load. Soil beneath a rolling wheel is likewise viewed as being in a steady plastic state similar to the failure occurring beneath a footing with inclined loading. Based on these assumptions, it is postulated that the load may be calculated using the generalized bearing capacity equation suggested by Meyerhof [10]. Meyerhof's equation, based on the well-known formula put forth by Terzaghi [11], accommodates the shape of the footing, embedment depth, and inclination of the loading utilizing so-called shape, depth, and inclination factors. With the factors listed in [12], the equation becomes

$$\begin{aligned}
 q_u = & cN_c \left(1 + \frac{B}{L} \frac{N_q}{N_c} \right) \left[1 + 0.4 \frac{D}{B} \right] \left(1 - \frac{2\beta}{\pi} \right)^2 \\
 & + \gamma DN_q \left(1 + \frac{B}{L} \tan \varphi \right) \left[1 + 2 \tan \varphi (1 - \sin \varphi)^2 \frac{D}{B} \right] \left(1 - \frac{2\beta}{\pi} \right)^2 \\
 & + 0.5 \gamma BN_\gamma \left(1 - 0.4 \frac{B}{L} \right) \left(1 - \frac{\beta}{\varphi} \right)^2
 \end{aligned} \tag{1}$$

where q_u is the average ultimate stress acting over the footing area, L is the length of a rectangular footing, $B < L$ is footing width, $D < B$ is embedment depth, c is cohesion, φ is the angle of internal friction, γ is unit weight, and β is the inclination angle of the load. The factors N_c , N_q and N_γ are functions of φ only and are listed in [12] as

$$N_q = \tan^2 \left(\frac{\pi}{4} + \frac{\varphi}{2} \right) e^{\pi \tan \varphi}; \quad N_c = (N_q - 1) \cot \varphi; \quad N_\gamma = 2(N_q + 1) \tan \varphi \tag{2}$$

The total force on the foundation, denoted Q , is found by multiplying the average stress q_u by the area of the footing. In the following, the area is assumed to be rectangular, such that the force is calculated simply as

$$Q = q_u BL \quad (3)$$

To move from the concept of limit load on a foundation to the indentation and rolling processes, the soil-wheel contact region is taken as an equivalent soil-footing contact face that evolves in area and shape as a function how far the wheel penetrates the soil (Figure 3). This assumption is warranted if the penetration of the wheel is small in relation to its diameter, as the curvature of the wheel plays a role with relatively deep penetration.

Indentation

The indentation process is illustrated in Figure 3a. As the wheel penetrates the soil, it displaces a certain amount of material. In terms of the contact area between the soil and wheel, this material is neglected, and the contact length h along the soil-wheel interface is therefore given by

$$h = 2\sqrt{ds - s^2} \quad (4)$$

where s is the penetration depth and d is the wheel diameter. The equivalent foundation parameters B and L are thus

$$\left. \begin{array}{l} B = h \\ L = b \end{array} \right\} \text{ for } h < b; \quad \left. \begin{array}{l} B = b \\ L = h \end{array} \right\} \text{ for } h \geq b \quad (5)$$

where b is the wheel width. The conditional dependence of B and L in Eq. (5), illustrated in Figure 3c, arises because $B < L$ in the bearing capacity formula.

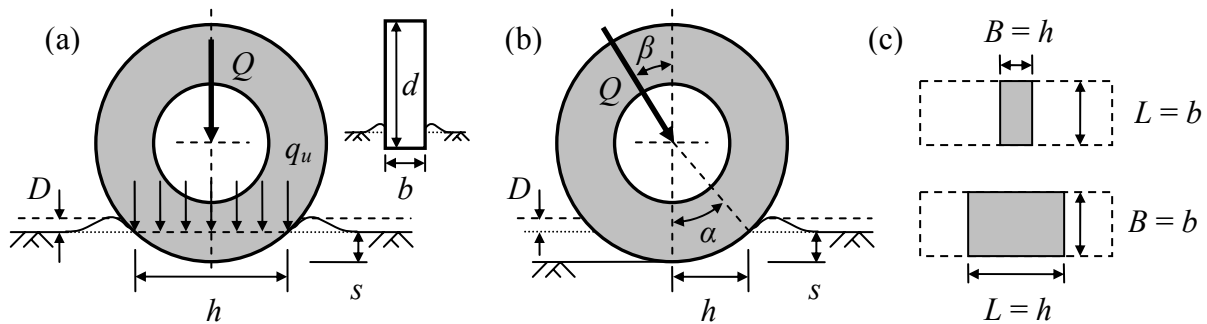


FIGURE 3 Wheel penetration process: (a) indentation; (b) rolling; (c) evolution of contact area with penetration depth.

The resistance added by displaced material is accounted for through the equivalent foundation depth D . In [3], an approximate expression for D was derived with $\varphi = 0$ by equating the displaced volume of material with the volume occupied by the wheel and assuming a mechanism for movement of material based loosely on the Prandtl solution. This expression is again used here, acknowledging that it is made somewhat more dubious for frictional materials exhibiting dilation/contraction:

$$D = \frac{1}{6}s \quad (6)$$

A more refined expression for D may be regarded as a potential improvement to the predictions obtained with this approach and will be addressed in future publications (e.g., [13]).

Substituting the equivalent foundation parameters L , B , and D from Eqs. (4)-(6) into Eqs. (1) and (3) gives the following lengthy, but straightforward, expressions for the wheel force as a function penetration depth:

$$\begin{aligned} Q_V = & 2b\sqrt{ds-s^2} \left\{ cN_c \left(1 + \frac{2\sqrt{ds-s^2}}{b} \frac{N_q}{N_c} \right) \left(1 + \frac{0.03s}{\sqrt{ds-s^2}} \right) \right. \\ & + 0.17\gamma s N_q \left(1 + 2 \frac{\sqrt{ds-s^2}}{b} \tan \varphi \right) \left[1 + \frac{0.17s \tan \varphi (1 - \sin \varphi)^2}{\sqrt{ds-s^2}} \right] \\ & \left. + \gamma \sqrt{ds-s^2} N_\gamma \left(1 - \frac{0.8\sqrt{ds-s^2}}{b} \right) \right\} \quad \text{for } 2\sqrt{ds-s^2} < b \end{aligned} \quad (7)$$

$$\begin{aligned} Q_V = & 2b\sqrt{ds-s^2} \left\{ cN_c \left(1 + \frac{0.5b}{\sqrt{ds-s^2}} \frac{N_q}{N_c} \right) \left(1 + \frac{0.07s}{b} \right) \right. \\ & + 0.17\gamma s N_q \left(1 + \frac{0.5b}{\sqrt{ds-s^2}} \tan \varphi \right) \left[1 + 0.33 \tan \varphi (1 - \sin \varphi)^2 \frac{s}{b} \right] \\ & \left. + \gamma b N_\gamma \left(0.5 - \frac{0.1b}{\sqrt{ds-s^2}} \right) \right\} \quad \text{for } 2\sqrt{ds-s^2} \geq b \end{aligned} \quad (8)$$

The angle β naturally vanishes in the indentation process. The indentation force is denoted Q_V for clarity in later sections, where $Q_V = Q \cos \beta$. The vertical component of force Q_V is associated with the weight acting on the wheel.

Rolling

In an advanced state of rolling, the contact area between the wheel and soil is reduced as compared with indentation, and the total force is inclined at the angle β (Figure 3b). Both have

the effect of reducing the wheel force for a given penetration depth. The effect of inclined loading is readily accommodated through the inclination factors in the bearing capacity formula.

The angle β must be known *a priori* in order to utilize Eq. (1). In this paper, β is assumed to bisect the angle α subtending the soil-wheel contact region. This assumption is discussed further in [3] and [13] and is based on experimental results in [14] and [15] that reveal, for a towed wheel, rough symmetry and antisymmetry of the normal and shear contact stresses, respectively, about the angle $\alpha/2$. Given these symmetries, β may be calculated as

$$\beta = \frac{\alpha}{2} = \frac{1}{2} \cos^{-1} \left(1 - 2 \frac{s}{d} \right) \approx \sqrt{\frac{s}{d}} \quad (9)$$

The approximation in Eq. (9) is valid for relatively small s/d (e.g., $s/d < 0.1$). The contact length h is taken as half of that for the case of indentation (Figure 3b). The resulting expression is

$$h = \sqrt{ds - s^2} \quad (10)$$

Using the same approximations as for indentation and taking the vertical component of force $Q_V = Q \cos \beta$ gives the following force-penetration relationships for rolling:

$$\begin{aligned} Q_V = b \sqrt{ds - s^2} \cos \left(\sqrt{\frac{s}{d}} \right) & \left\{ c N_c \left(1 + \frac{\sqrt{ds - s^2}}{b} \frac{N_q}{N_c} \right) \left[1 + \frac{0.07s}{\sqrt{ds - s^2}} \right] \left(1 - 0.64 \sqrt{\frac{s}{d}} \right)^2 \right. \\ & + 0.17 \gamma s N_q \left(1 + \frac{\sqrt{ds - s^2}}{b} \tan \varphi \right) \left[1 + \frac{0.33s \tan \varphi (1 - \sin \varphi)^2}{\sqrt{ds - s^2}} \right] \left(1 - 0.64 \sqrt{\frac{s}{d}} \right)^2 \\ & \left. + \gamma \sqrt{ds - s^2} N_\gamma \left(0.5 - \frac{0.2 \sqrt{ds - s^2}}{b} \right) \left(1 - \frac{1}{\varphi} \sqrt{\frac{s}{d}} \right)^2 \right\} \quad \text{for } 2\sqrt{ds - s^2} < b \end{aligned} \quad (11)$$

$$\begin{aligned} Q_V = b \sqrt{ds - s^2} \cos \left(\sqrt{\frac{s}{d}} \right) & \left\{ c N_c \left(1 + \frac{b}{\sqrt{ds - s^2}} \frac{N_q}{N_c} \right) \left[1 + \frac{0.07s}{b} \right] \left(1 - 0.64 \sqrt{\frac{s}{d}} \right)^2 \right. \\ & + 0.17 \gamma s N_q \left(1 + \frac{b \tan \varphi}{\sqrt{ds - s^2}} \right) \left[1 + 0.33 \tan \varphi (1 - \sin \varphi)^2 \frac{s}{b} \right] \left(1 - 0.64 \sqrt{\frac{s}{d}} \right)^2 \\ & \left. + \gamma b N_\gamma \left(0.5 - \frac{0.2b}{\sqrt{ds - s^2}} \right) \left(1 - \frac{1}{\varphi} \sqrt{\frac{s}{d}} \right)^2 \right\} \quad \text{for } 2\sqrt{ds - s^2} \geq b \end{aligned} \quad (12)$$

RESULTS

Eqs. (7) and (8) for indentation and Eqs. (11) and (12) for rolling give approximate analytic expressions for the wheel weight Q_V in terms of the soil properties (φ , c and γ), wheel geometry

(b and d), and penetration depth (s). These relationships are plotted in Figure 4 for some example data. The force-penetration curves are strongly nonlinear, and the formulas predict that for a given wheel weight a rolling wheel will penetrate much deeper than an indenting wheel.

Given the simplicity of the approach presented in this paper, one may be justified in regarding the derived formulas as somewhat speculative. For this reason, the predictions are compared with results obtained from numerical simulation using the finite element method, as well as experimental data.

In [3] and [4], approaches for simulating three-dimensional indentation and rolling processes using the commercial code ABAQUS/Explicit were presented for the case of purely cohesive soil ($\varphi = 0$). Similar numerical simulations were performed for comparison with the formulas for frictional soil ($\varphi > 0$) presented in this paper. The only difference between the simulations performed for this paper and those discussed in [3] and [4] is the material model used for the soil. The bearing capacity formula is based on the Mohr-Coulomb yield condition and associated plastic flow. In the simulations, the soil was modeled as an elastic-perfectly plastic material obeying the extended Drucker-Prager yield condition available in ABAQUS/Explicit [16], which may be regarded as a smooth counterpart of the Mohr-Coulomb yield condition. The procedure discussed in [16] was used to match the Drucker-Prager parameters with the Mohr-Coulomb parameters in triaxial response (extension and compression), as much as the model is capable of doing. Non-associated plastic flow (dilation angle equal to zero) was assumed. In the simulation results presented here, the Young's modulus of the soil was fixed at 40 MPa (5800 psi), the Poisson's ratio was 0.3, and the coefficient of friction between the wheel and soil was 0.5.

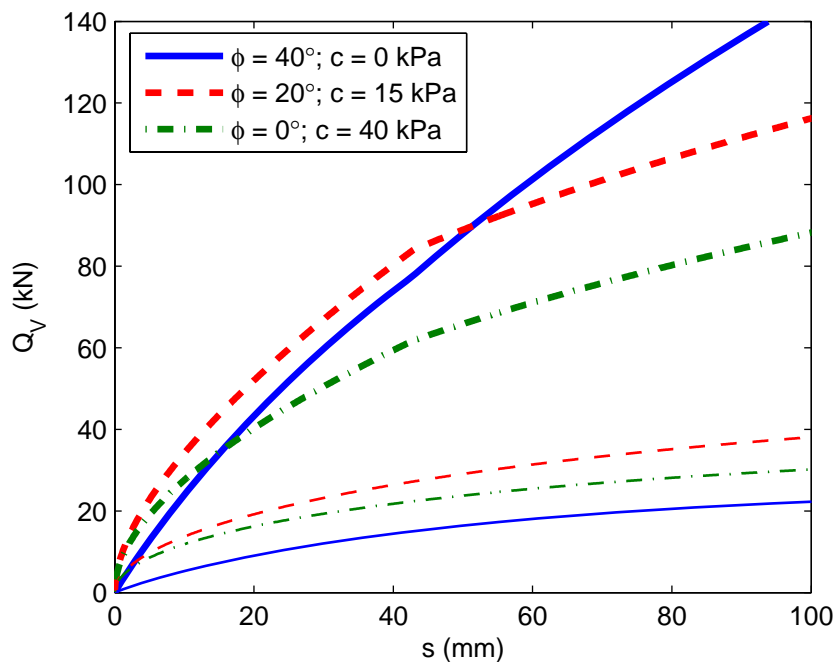


FIGURE 4 Example force-penetration curves (thick lines for indentation and thin lines for rolling; $d = 1.5$ m, $b = 0.5$ m, and $\gamma = 18$ kN/m³).

Figure 5 compares the results obtained from the ABAQUS simulations with the predictions from the formulas presented in this paper for a cohesive-frictional soil with $\phi = 30^\circ$ and $c = 25$ kPa (3.6 psi). The results are in astonishing agreement, given the approximate nature of the derived formulas. Not surprisingly, the predictions for indentation exhibit better agreement, as somewhat stronger assumptions are introduced to arrive at the formulas for rolling (namely with respect to inclination of the loading).

Predictions from Eqs. (11) and (12) are also compared to experimental data from [3] and [13], in which small-scale rolling tests were conducted on dry, dense sand and nearly-saturated clay ([3] pertains only to the clay material). Details regarding soil properties, test setup, and procedures may be found in these references. The strength parameters ϕ and c for these soils were deduced from triaxial compression tests, the results of which are in Figure 6. As shown, a best-fit linear failure envelope for the dense sand is characterized by some apparent cohesion, which appears to be an artifact arising from nonlinearity of the true envelope. A linear envelope characterized by $c = 0$ corresponds to $\phi \approx 46^\circ$. Triaxial compression tests on the clay revealed $c = 28.5$ kPa (4.13 psi) and $\phi = 4^\circ$.

Figures 7 and 8 show the wheel force-penetration data collected in [3,13] for wheels operating in the sand and clay, respectively. In the laboratory, small ($d \sim 100$ mm, 4 in.) aluminum wheels with roughened contact surfaces were rolled through a bed of soil in the towed condition. The wheels were constrained to move through the soil bed at constant depth s , and vertical force Q_V at an advanced stage of rolling was then measured with a load cell. As noted in [3], the cohesion of the clay soil had increased roughly 25 percent, due to aging and some moisture loss, between the times when the triaxial compression tests were performed and the rolling tests were conducted, as determined from unconfined compression tests. A corrected value of cohesion is used in the theoretical predictions.

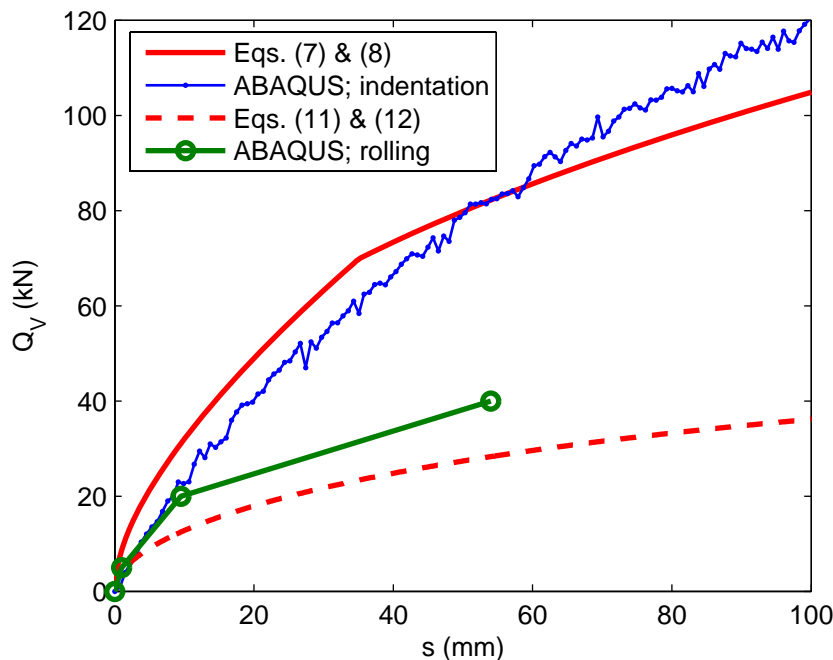


FIGURE 5 Comparison of force-penetration curves from derived formulas and results from ABAQUS simulations ($\phi = 30^\circ$, $c = 25$ kPa, $\gamma = 18$ kN/m³, $d = 1.52$ m, and $b = 0.46$ m).

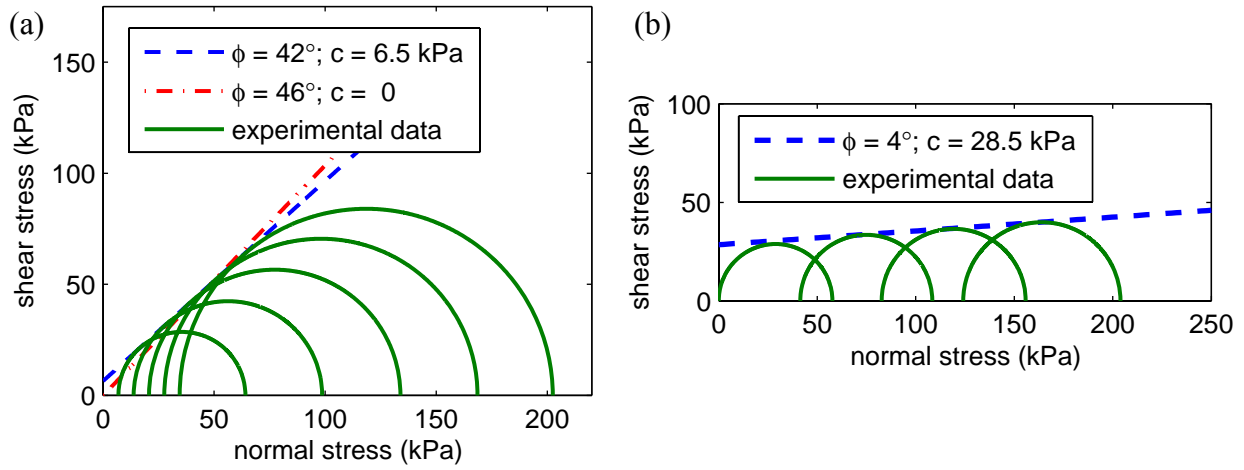


FIGURE 6 Mohr's plots for (a) dense sand and (b) clay determined from triaxial tests [13].

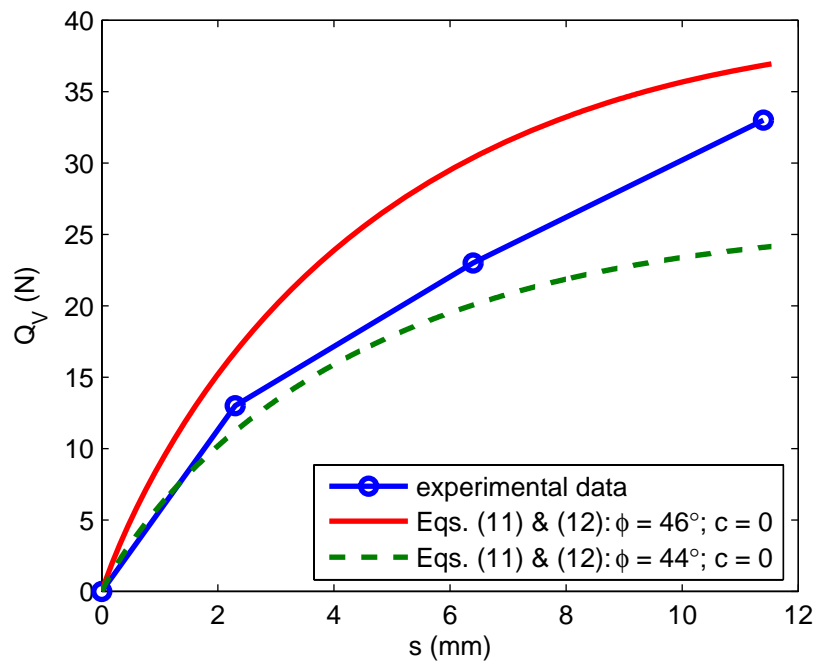


FIGURE 7 Comparison of predictions and experimental data from small-scale tests of rolling wheel on sand ($d = 115$ mm, $b = 38$ mm, and $\gamma = 17.4$ kN/m³).

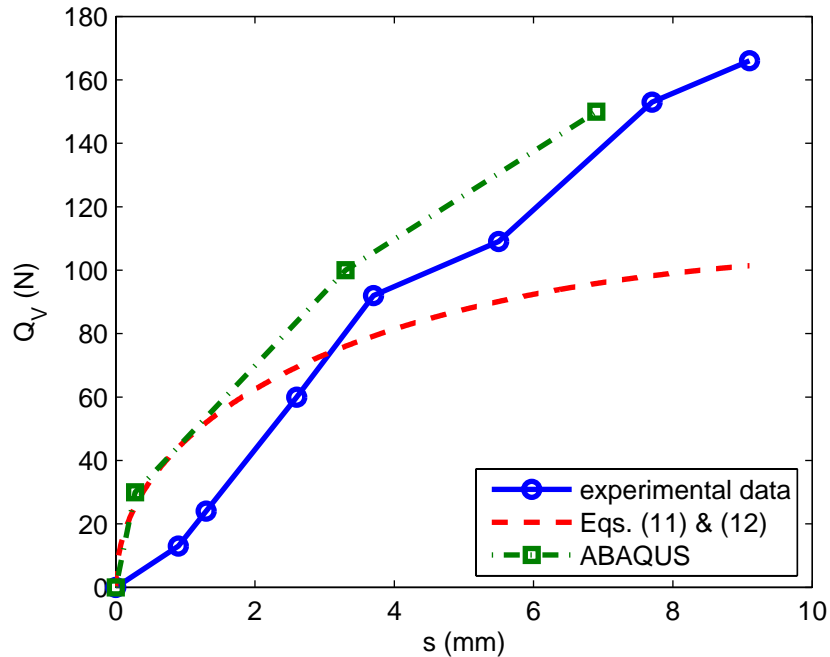


FIGURE 8 Comparison of predictions and experimental data from small-scale tests of rolling wheel on clay ($d = 78$ mm, $b = 25$ mm, $\phi = 4^\circ$, and $c = 36$ kPa; ABAQUS simulation results from [3]).

For the sand (Figure 7), the predicted force-penetration curves match the experimental data quite well. To reflect the ambiguity in measured ϕ , two predicted curves are plotted, using $\phi = 44^\circ$ and $\phi = 46^\circ$. The difference in predictions arising from a mere 2° change in friction angle reveals the high level of sensitivity to this strength parameter. Despite the uncertainty in how ϕ should be most appropriately chosen, it is clear that the theoretical models give reasonable results. Predictions for the clay soil (Figure 8) are somewhat worse as compared with experiments, with deviations at both small and large relative values of penetration. The trends in data, however, are again characterized fairly well by the theoretical models. Potential reasons for the discrepancies between the predictions and experimental data are discussed in [3,13], where theoretical means for rectifying the formulas by modifying the inclination factors are also proposed.

Force-penetration relationships as such are not of particular interest in test rolling, since the force or weight of the test roller is invariably held constant. Of more relevance are plots like the one shown in Figure 9, which relates, for a rolling wheel, measured penetration s to the soil strength parameters ϕ and c for fixed test roller parameters. Corresponding to the device in [2], the test roller parameters are taken as $Q_V = 134$ kN (15 tons), $d = 1.52$ m (60 in.) and $b = 0.46$ m (18 in.). The derived formulas, although implicit with respect to material properties, may be easily solved numerically to generate such plots. Figure 9 reveals the extent of nonlinear variation in penetration with respect to soil strength. A small increase in cohesion or internal friction (e.g., through compaction) can reduce the penetration drastically.

Also shown in Figure 9 for comparison are the rut depths determined from several ABAQUS simulations. Qualitatively, the results agree very well. For highly frictional materials ($\phi \geq 30^\circ$), there is even quantitative agreement. For cohesive materials ($\phi < 20^\circ$), the disparity between predictions using the formulas and the simulation results can be rather large. This is consistent with the observed differences between predictions and experimental data for the clay soil (Figure 8).

The derived formulas can be readily used to investigate the effect of varying test roller parameters. For example, the test roller wheel weight of 134 kN (15 tons) specified in [2] is considered by some to be prohibitively large. Figure 10 is a reproduction of Figure 9, except that the weight is halved to 67 kN (7.5 tons). The curves are shifted downwards by significantly more than a factor of two. The test roller ultimately becomes more sensitive to weaker soils, in the sense that regions of steep gradients within the plot are relocated to areas with lower ϕ and c .

Because the soil is characterized by two strength parameters, the properties of the soil cannot be uniquely determined by one measurement of penetration. It may be practical to resolve this issue by employing two test roller wheels with varying characteristics (e.g., different wheel weights), although this aspect of the test rolling problem is not pursued further here. Note also that the unit weight of the soil γ is practically unimportant, with the exception of cohesionless soils, for which the models predict that Q_V scales linearly with γ .

CONCLUDING REMARKS

The formulas developed in this paper may be used as a basis for relating penetration depth of an indenting or rolling wheel to the angle of internal friction and cohesion of a soil, given the wheel geometry and weight acting on the wheel. The expressions are algebraic and may be easily manipulated to investigate relevant aspects of test rolling such as sensitivity. The formulas provide compelling agreement with results from laboratory experiments and three-dimensional numerical simulation using the finite element code ABAQUS, although the predictions should ultimately be compared with data from field experiments. While there is room for improving accuracy, the formulas capture the trends shown in numerical and experimental results. Accuracy may be improved by, among other things, incorporating more accurate factors in the generalized bearing capacity formula (e.g., N_γ , shape factors, and inclination factors), as the bearing capacity formula is itself approximate.

The present analysis is limited to the case of a rigid, right-cylindrical wheel, although wheel flexibility and other geometries can be managed within the same framework (cf. [3]). A rigid wheel is most desirable for the purpose of test rolling, although a method allowing for wheel flexibility may be necessitated by the practical appeal of pneumatic tires. Also, it is tacitly assumed in this paper that the soil is homogeneous or, more specifically, that the uppermost layer of soil is sufficiently thick that differences in underlying layers have no influence. Preliminary results from numerical simulation indicate that for the Minnesota test roller, the presence of weak or strong layers 0.7 m (28 in.) or more below grade has minimal effects on wheel penetration [13].

The angle of internal friction and cohesion of base and subgrade materials are themselves not typically used in roadway design. It may be possible, however, to interpret them in terms of parameters more familiar to practitioners. For example, Ayers *et al.* [17] found a strong correlation between the angle of internal friction and penetration rate of a dynamic cone penetrometer (DCP), which is a tool commonly used in practice for quality assurance. Given such a correlation, test roller results may be considered analogous to a continuous record of DCP penetration rate along a roadway. In this light, test rolling is a rather attractive test method, since a single DCP test is time consuming to conduct. Likewise, cohesion has been shown to bear a relationship with the Atterberg limits and moisture content of cohesive soils (cf. [18]), and whereas cohesion may not be relevant to roadway designers, the Atterberg limits are perhaps more amenable for use, playing an integral part in the widely used soil classification systems.

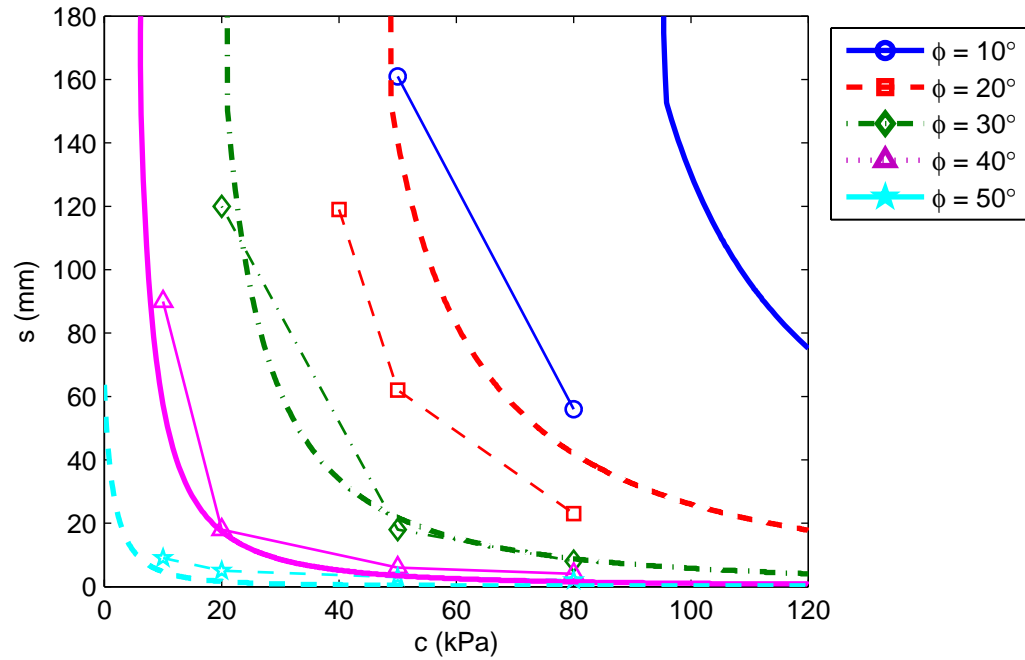


FIGURE 9 Relation between penetration depth and strength parameters for rolling wheel with $Q_V = 134$ kN, $d = 1.52$ m, $b = 0.46$ m, and $\gamma = 18$ kN/m³ (smooth curves are from derived formulas; connected points show results from ABAQUS simulations).

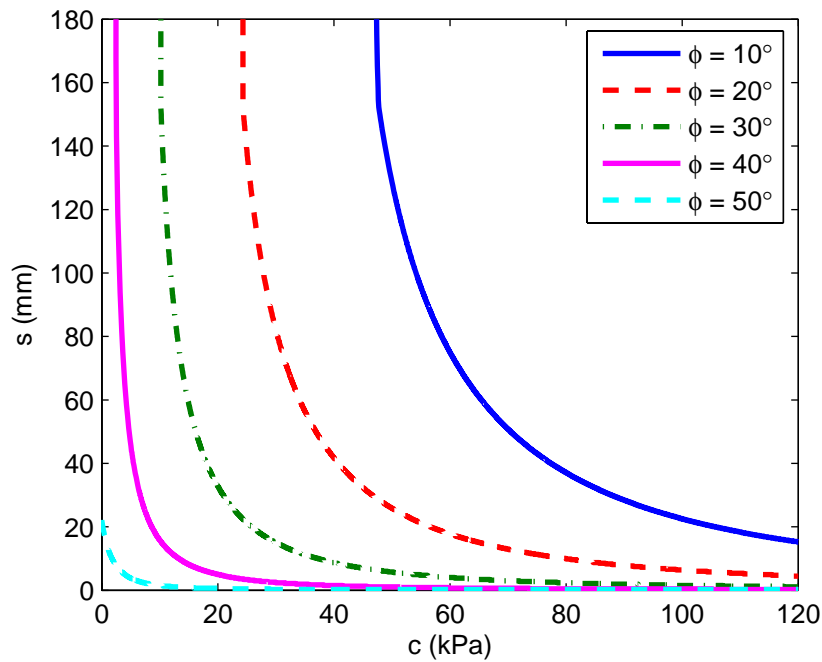


FIGURE 10 Relation between penetration depth and strength parameters for rolling wheel with $Q_V = 67$ kN, $d = 1.52$ m, $b = 0.46$ m, and $\gamma = 18$ kN/m³.

ACKNOWLEDGEMENT

Support provided by the Minnesota Local Road Research Board and the Shimizu Corporation is gratefully acknowledged. Computer resources provided by the University of Minnesota Supercomputing Institute are appreciatively recognized.

REFERENCES

1. Crovetto, J. A. *Comprehensive Subgrade Deflection Acceptance Criteria - Executive Summary*. Report No. WI/SPR-05-02. Wisconsin Department of Transportation, Madison, 2002.
2. *Standard Specifications for Construction*. Specification 2111. Minnesota Department of Transportation, St. Paul, 2000.
3. Hambleton, J. P. *Modeling Test Rolling in Clay*. MS Thesis. University of Minnesota, Minneapolis, 2006.
4. Hambleton, J. P., and A. Drescher. Modeling Test Rolling on Cohesive Subgrades. *Proceedings of the International Conference on Advanced Characterisation of Pavement and Soil Engineering Materials*, Athens, Vol 1., Balkema, Rotterdam, 2007, pp. 359-368.
5. Bekker, M. G. *Off-the-Road Locomotion*. University of Michigan Press, Ann Arbor, 1960.
6. Bekker, M. G. *Introduction to Terrain-Vehicle Systems*. University of Michigan Press, Ann Arbor, 1969.
7. Karafiath, L. L., and E. A. Nowatzki. *Soil Mechanics for Off-Road Vehicle Engineering*, Trans Tech Publications, Clausthal, 1978.
8. Wong, J. Y. *Terramechanics and Off-Road Vehicles*. Elsevier, New York, 1989.
9. Wong, J. Y. *Theory of Ground Vehicles*. Wiley, New York, 2001.
10. Meyerhof, G. G. Some Recent Research on Bearing Capacity of Foundations. *Canadian Geotechnical Journal*, Vol. 1, No. 1, 1963, pp. 16-26.
11. Terzaghi, K. *Theoretical Soil Mechanics*. Wiley, New York, 1943.
12. Das, B. M. *Fundamentals of Geotechnical Engineering*. Thomson, Toronto, 2005.
13. Hambleton, J. P., and A. Drescher. *Development of Improved Test Rolling Methods for Roadway Embankment Construction - Final Report*. Minnesota Department of Transportation, Research Services Section, St. Paul, (In Preparation).

14. Onafeko, O., and A. R. Reece. Soil Stresses and Deformations Beneath Rigid Wheels. *Journal of Terramechanics*, Vol. 4, No. 1, 1967, pp. 59-80.
15. Krick, G. Radial and Shear Stress Distribution Under Rigid Wheels and Pneumatic Tires Operating on Yielding Soils with Consideration of Tire Deformation. *Journal of Terramechanics*, Vol. 6, No. 3, 1969, pp. 73-98.
16. *ABAQUS Version 6.6 Documentation*. ABAQUS, Inc., Providence, 2006.
17. Ayers, M. E., M. R. Thompson, and D. R. Uzarski. Rapid Shear Strength Evaluation of In Situ Granular Materials. In *Transportation Research Record: Journal of the Transportation Research Board*, No. 1227, TRB, National Research Council, Washington, D.C., 1989, pp. 134-146.
18. Sharma, B., and P. K. Bora. Plastic Limit, Liquid Limit and Undrained Shear Strength of Soil—Reappraisal. *Journal of Geotechnical and Geoenvironmental Engineering*, Vol. 129, No. 8, 2003, pp. 774-777.